Computational Study of the Vibrational Spectra of α- and β-Keggin Polyoxometalates

Adam J. Bridgeman*[a]

Abstract: The structures and vibrational frequencies of the α- and β-isomers of the phosphomolybdate Keggin anion $[PMo_{12}O_{40}]^{3-}$ have been calculated by using density functional theory. Good agreement between the calculated unscaled vibrational frequencies and those determined experimentally and between the calculated and observed IR traces has been obtained allowing the IR and Raman spectra to be assigned. For the α-isomer, the agreement with experiment using the current level of theory is superior to that obtained previously. For the β-isomer, for which no non-empirical study has previously been reported, the agreement with experiment is slightly poorer but still allows the spectrum to be assigned unambiguously. To calculate the structure and vibrational spectra of these large molydate cluster ions requires large basis sets and a good treatment of electron correlation and relativistic effects. For the 53-atom $[PMo_{12}O_{40}]^{3-}$ ions, the computational demands are very high, requiring several months computational time. The calculated IR spectral traces for the two isomers are quite similar due to the relative flexibility of the molybdates, where the slight weakening of the bonding of the rotated trimetallic unit to the rest of the cluster in the β-isomer is compensated by contraction of the bonds within the unit, and the structure of the $[MO_6]$ and $[PO_4]$ units in the two isomers is nearly identical. The vibrations characteristic of the bridging Mo-O-Mo bonds involve both the "2–2" junctions between rotated $[M_3O_{13}]$ units and the "1–2" junctions between rotated and unrotated units. The separation of "ligand" and "interligand" vibrations is not clear. The vibrational analyses confirm the high symmetry, namely T_d and C_{3v} for the α- and β-isomers, respectively, assumed by previous workers in this field. The characteristic group frequencies for the Type I polyoxometalates containing both edge- and corner-sharing I octahedra have been identified.

Keywords: density functional calculations · Keggin anions · polyoxometalates · vibrational spectroscopy

Introduction

The polyoxometalates constitute an extremely large and diverse class of compounds.[1,2] Their remarkable chemical and physical properties have led to a variety of potential applications in medicine, catalysis, solid-state technology, and chemical analysis.[3,4] Polyoxometalates are primarily built by edge- and, occasionally, corner-sharing of MO_6 octahedra and the resulting cages are usually approximately spherical. Heteropolyoxometalates have a general chemical formula $[X_nM_pO_q]^{z-}$, where M is most commonly Mo or W, and X is a main-group or transition-metal heteroatom. The most important heteropolyoxometalates are undoubtably the Keggin anions that have the formula $[XM_{12}O_{40}]^{z-}$. The first polyoxometalate, $[PMo_{12}O_{40}]^{3-}$, was reported in 1826 by Berzelius.[5] In 1864, two isomeric forms, now known as the α- and β-isomers, of $[H_4SiMo_{12}O_{40}]$ were observed by Marignac.[6]

The structure of the α-isomer of $[PW_{12}O_{40}]^{3-}$ was solved in 1933 by Keggin.[7] Figure 1a shows the α-Keggin structure as an assemblage of (distorted) $[MO_6]$ octahedra and a $[XO_4]$ tetrahedron. The ion exhibits ideal T_d symmetry and all M atoms are equivalent. The $[MO_6]$ units are edge-shared into four C_{3v} $[M_3O_{13}]$ groups and these 'ligands' are connected to the threefold axes of the central $[XO_4]$ tetrahedron to give the molecular symmetry. As shown in Figure 1b, the metal atoms occupy the centers of distorted C_s octahedra with one terminal M–O_t bond. The M–O_{4c} bonds are *trans*-orientated with respect to the terminal M–O_t bonds and feature four-coordinate oxygen atoms. The M–O_{2c1} bonds and Mo–O_{2c2} bonds are *cis*-orientated with respect to the M–O_t bonds and feature two-coordinate oxygen atoms. The M–O_{2c1} bonds connect the $[MO_6]$ octahedra into $[M_3O_{13}]$ groups. The M–O_{2c2} bonds connect the $[M_3O_{13}]$ units together to form twelve equivalent "2–2" junctions

[a] Dr. A. J. Bridgeman
Department of Chemistry, University of Hull
Kingston-upon-Hull, HU6 7RX (UK)
E-mail: a.j.bridgeman@hull.ac.uk

Supporting information for this article is available on the WWW under http://www.chemeurj.org/ or from the author. Full lists of all the calculated frequencies and description of the vibrational modes for α and β-$[PMo_{12}O_{40}]^{3-}$.

 DOI: 10.1002/chem.200305781

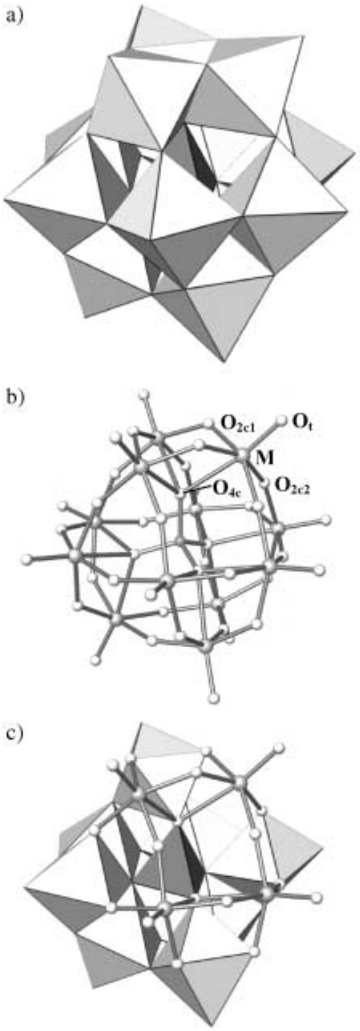

Figure 1. Structure and atom-labeling scheme for a α-Keggin anion showing a) the assemblage of twelve $[MO_6]$ octahedra and a $[XO_4]$ tetrahedron, b) individual atoms and bonds, c) the "2–2" junctions between $[M_3O_{13}]$ units.

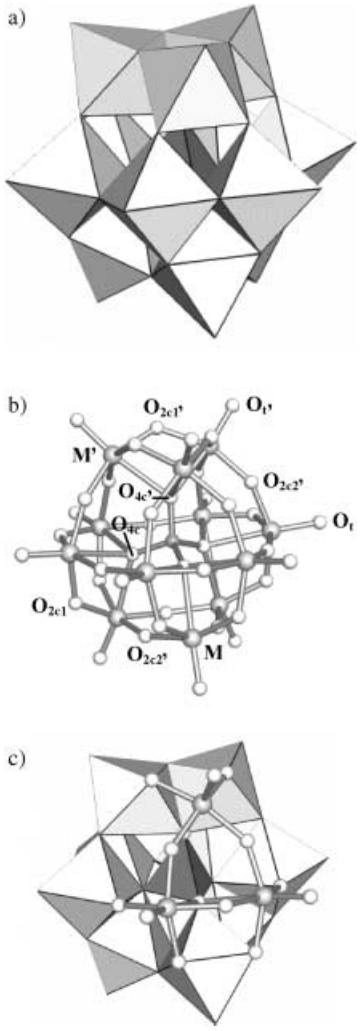

Figure 2. Structure and atom-labeling scheme for a β-Keggin anion showing a) the assemblage of twelve $[MO_6]$ octahedra and a $[XO_4]$ tetrahedron, b) individual atoms and bonds, c) the "1–2" junctions between the rotated and unrotated $[M_3O_{13}]$ units.

with two metal atoms of one unit connected through the bridging oxygen atoms to two metal atoms in another group (Figure 1c).

β-Isomers appear to be much less common. The structure of β-$[SiW_{12}O_{40}]^{4-}$ was first determined by crystallography in 1973 by Yamamura and Sasaki,[8] and the β-structure has only been proven by X-ray crystallography for a handful of systems. The β-isomer structure, shown in Figure 2a in polyhedral representation and in Figure 2b with atoms and bonds, may be considered as derived from the α-structure by rotation of one $[M_3O_{13}]$ group by 60° about its threefold axis to give a structure with C_{3v} symmetry. The six connections between the rotated $[M_3O_{13}]$ group, shown in Figure 2c, and the other groups are "1–2" junctions with a common metal atom in the rotated group connected by bridging oxygen atoms to a two metal atoms in the unrotated group.

Vibrational spectroscopy is able to detect small structural differences and has potential as a probe of the structures and dynamics of Keggin anions.[9–11] However, the assignment of the vibrational spectra of clusters such as Keggin anions is problematic and complicated due to both their large size and structural complexity. In comparison to the extensive literature on the chemistry, properties, and applications of Keggin anions, relatively few high-level computational studies have been reported.[12–18] I have recently completed detailed computational studies of the vibrational frequencies and assignments of Lindqvist[19] and α-Keggin[18] anions. In the study of the Lindqvist anions, the effects of the computational method—basis set and density functional—were examined. Vibrational analyses on large anions such as these are extremely computationally demanding, requiring accurate geometries and treatment of electron correlation and relativistic effects. The Hartree–Fock method, for example, is able to reproduce the geometries of these anions quite well but performs very poorly when applied to vibrational frequencies. Herein, I report the first nonempirical comparison of the vibrational frequencies of α- and β-Keggin anions which, as detailed below, has required an even larger computational effort.

Computational Approach

In our previous study of the vibrational spectra of Lindqvist isopolyanions,[19] we examined the performance of a variety of computational methods. The results suggested that the local density approximation (LDA) with triple-ζ Slater-type orbitals (STO) and the ZORA relativistic approach implemented within the ADF program[20,21] is best able to model both the structure and vibrational spectra of these polyanions when treated as pseudo-gas phase species. However, the ADF program uses numerical differentiation of analytic first derivatives of the energy to calculate vibrational frequencies. This approach requires a large number of single point calculations at geometries close to the equilibrium structure, requiring high SCF convergence and integration accuracy for 53-atom structures with no symmetry. In my recent work on the vibrational spectra of α-Keggin anions,[18] this approach proved to be too computationally demanding to be applied to a systematic comparison of the effect of metal ion, heteroatom and cluster charge and instead I utilized the analytical second derivatives available in the Gaussian 98[22] program. Unfortunately, the smaller basis sets and poorer treatment of relativistic effects available for programs based on Gaussian-type orbitals led to severe problems when applied to the β-Keggin isomers and it proved not to be possible to successfully converge sufficiently accurate structures for vibrational analyses. As a result, the calculations reported here have been performed by using the ADF approach which has previously been shown to provide accurate structures for β-Keggin anions[13] as well as the best results for the vibrational spectra of Lindqvist anions.[19] Due to the computational demands, the comparison has been restricted to α- and β-$[PMo_{12}O_{40}]^{3-}$. The computational approach suggested to be most accurate for the Lindqvist anions has been used with triple-ζ STO (ADF type TZ1P) on all atoms incorporating frozen cores (ADF type Mo.3d, O.1 s, and P.2p) and the ZORA relativistic approach[20] and the Vosko–-Wilk–Nusair (VWN) form of the local density approximation.[23]

Spectral traces have been plotted by using 'spectralPlot'[24] assuming Lorentzian band shapes and with an average band width chosen to reflect that found experimentally.

Results

Structures of the α- and β-isomers of $[PMo_{12}O_{40}]^{3-}$: Table 1 lists optimized M–O and X–O bond lengths together with the available experimentally determined distances[25,26] for the α- and β-isomers of $[PMo_{12}O_{40}]^{3-}$. The vibrational analyses reported below for α- and β-$[PMo_{12}O_{40}]^{3-}$ confirm that these isomers have full T_d and C_{3v} symmetry, respectively, in the gas phase, as assumed in earlier computational studies of the structures of these anions.[13] For the α-isomer, the agreement between the calculated and experimentally determined bond lengths is good and slightly better than that reported previously,[13] with significant improvement on the geometry used for my previous vibrational analysis[18] of this anion. The crystal structure of the β-form of this phosphomolybdate has not been reported. Only small differences in the geometries of the $[MO_6]$ and $[PO_4]$ polyhedra are observed in the α- and β-isomers. The $[PO_4]$ unit suffers a slight trigonal compression in the β-form, suggesting a small decrease in its interaction with the rotated $[M'_3O_{13}]$ group leading to a lengthening of the $M'–O_{4c}$ bonds. This weakened interaction is presumably compensated by the slight contraction of the $M'–O_{2c1'}$ and $M'–O_t$ bonds. The interaction of the rotated group with the other $[M_3O_{13}]$ units is also weakened with slightly longer $M'–O_{2c2'}$ bonds. The bonding in the unrotated $[M_3O_{13}]$ units does not appear to be greatly affected by the lowering of the symmetry between the α- and β-forms.

Table 1. Calculated bond lengths [Å] for the α- and β-isomers of $[PMo_{12}O_{40}]^{3-}$. The atom numbering is defined in Figure 1 and 2 with primed atoms located on the rotated $[M_3O_{13}]$ unit of the β isomer. The averaged experimental[25,26] bond lengths for α-$[PMo_{12}O_{40}]^{3-}$ are shown in parenthesis. The bond lengths involving the unprimed atoms in the β isomer are mean values for the various bond types.

Bond	$[PMo_{12}O_{40}]^{3-}$	
	α	β
$X–O_t$	1.554 (1.53)	1.555
$X–O_{t'}$		1.550
$M–O_t$	1.706 (1.69)	1.706
$M'–O_{t'}$		1.705
$M–O_{4c}$	2.419 (2.40)	2.419
$M'–O_{4c'}$		2.436
$M–O_{2c1}$	1.917 (1.96)	1.919
$M'–O_{2c1'}$		1.914
$M–O_{2c2}$	1.907 (1.88)	1.905
$M–O_{2c2'}$		1.910
$M'–O_{2c2'}$		1.915

Vibrational spectra of the $[PMo_{12}O_{40}]^{3-}$ α- and β-Keggin anions: A Keggin $[XMo_{12}O_{40}]^{z-}$ ion has 153 normal modes of vibration. For the tetrahedral symmetry of the α-isomer, these span the range given in Equation (1), where the IR and Raman (R) activities are shown in parenthesis. Forty-four Raman bands ($9a_1 + 13e + 22t_2$) and twenty-two infrared ($22t_2$ coincident with $22t_2$ Raman bands) might be expected in the vibrational spectrum.

$$\Gamma_{vib}(\alpha) = 9a_1\ (R) + 4a_2 + 13e\ (R) + 16t_1 + 22t_2\ (IR,\ R) \quad (1)$$

For the C_{3v} symmetry of the β-isomer, the vibrational modes span the range given in Equation (2), where the IR and Raman activities are again shown in parenthesis.

$$\Gamma_{vib}(\beta) = 31a_1\ (IR,\ R) + 20a_2 + 51e\ (IR,\ R) \quad (2)$$

Eighty-two coincident IR and Raman bands might be expected in the vibrational spectrum. The sixteen inactive t_1 modes of the α-isomer are split into $16a_2 + 16e$ for the β-isomer by the descent in symmetry with the latter becoming both IR and Raman active. The twenty-two IR and Raman active t_2 modes of the α-isomer are similarly split into $22a_1 + 22e$ modes for the β-isomer. The $9a_1 + 13e$ modes of the α-isomer become IR-active in the β-form. The vibrational spectra of Keggin anions have been reported by a number of workers.[9–11] The most comprehensive experimental studies have been completed by Rocchiccioli-Deltcheff and coworkers including comparisons of Keggin anions with different cations[9] and heteroatoms,[9,10] and studies of the effect of isomerism.[10] In this work, calculated frequencies correspond to pseudo-gas phase anions and are compared to the experimental IR and Raman values reported by Rocchiccioli-Deltcheff et al.[9,10] with the large, weakly coordinating cation $[N(n\text{-}C_4H_9)_4^+]$ (TBA), which was considered by these workers to minimize the effects of anion–anion interactions on the spectra.

The assignment of the vibrational spectra of the α-isomers of $[PMo_{12}O_{40}]^{3-}$, $[PW_{12}O_{40}]^{3-}$, $[AsMo_{12}O_{40}]^{3-}$, $[SiMo_{12}O_{40}]^{4-}$, $[GeMo_{12}O_{40}]^{4-}$, $[AlMo_{12}O_{40}]^{5-}$, and $[GaMo_{12}O_{40}]^{5-}$ has been reported previously using the results of density functional calculations with quasi-relativistic effective core potentials to represent the atomic cores and double-ζ quality Gaussian type orbitals (GTO) for the valence orbitals together with Becke's three parameter hybrid functional B3LYP.[18]

Table 2 lists the calculated and experimental frequencies and assignments for the assigned bands of α-$[PMo_{12}O_{40}]^{3-}$ from the present STO study, together with calculated intensities. A full list of calculated frequencies and a description of the nature of the vibrations is available in the Supporting Information. As indicated by our previous work on the structures and vibrational frequencies of Lindqvist isopolyanions,[19] the computational method used in the present work leads to a significantly improved modeling of the observed vibrational frequencies of α-$[PMo_{12}O_{40}]^{3-}$ compared to that obtained at the B3LYP-GTO level. The root mean square (RMS) error between the calculated and experimental frequencies is reduced from 26 cm^{-1} in the GTO study to 20 cm^{-1} in the present STO study for twenty-two assigned IR and Raman bands. Figure 3a shows a graphical comparison between the calculated IR spectrum and that observed experimentally.[10] The observed trace has been constructed by converting the published spectrum of Thouvenot et al.[10] from transmittance to relative absorbance, assuming 5% transmittance for the strongest bands. The calculated trace has been constructed from the calculated frequencies and intensities using Lorentzian band shapes. Although a more exacting test of the calculated results than the frequencies, the major features of the experimental trace are reproduced satisfactorily, particularly in the region above 800 cm^{-1} characterized by strong bands associated with Mo-O and P-O stretching motions.

Table 2. Calculated and experimental vibrational frequencies (in cm^{-1}) and approximate descriptions for the assigned bands of α-$[PMo_{12}O_{40}]^{3-}$. The calculated IR intensities [km mol^{-1}] and an indication (vs = very strong, s = strong, m = medium, w = weak, vw = very weak, sh = shoulder) of the relative intensity in the experimental IR and Raman spectra is also given.

Mode		Calcd	Observed[9,10]		Assignment
			IR	Raman	
t_2	ν_{43}	1053 (340)	1063 (m)		ν_{as}(P–O), ν_{as}(Mo–O_t) (asymmetric coupling)
a_1	ν_1	1016		986 (vs)[a]	ν_s(Mo–O_t)
t_2	ν_{44}	998 (640)	965 (sh)	964 (m)	ν_{as}(Mo–O_t)
e	ν_{14}	973		971 (sh)	ν_{as}(Mo–O_t)
t_2	ν_{45}	972 (880)	955 (vs)		ν_{as}(P–O), ν_{as}(Mo–O_t) (symmetric coupling)
t_2	ν_{46}	904 (195)	880 (s)	894 (w)	ν_{as}(Mo-O_{2c2}-Mo)
t_2	ν_{47}	806 (1625)	805 (vs)		ν_{as}(Mo-O_{2c1}-Mo)
a_1	ν_3	631		603 (m)[a]	ν_s(Mo-O_{2c1}-Mo), δ(Mo-O_{2c1}-Mo)
t_2	ν_{51}	479 (24)	464 (w)	465 (vw)	δ(Mo-O_{2c2}-Mo)
a_1	ν_5	420		451 (vw)	δ(Mo-O_{2c1}-Mo)
t_2	ν_{53}	401 (178)	386 (s)	370 (vw)	δ(Mo-O_{2c2}-Mo)
t_2	ν_{57}	239 (10)		255 (w)	δ(O_{2c1}-Mo-O_{2c1}), δ(O_{2c2}-Mo-O_{2c2})
e	ν_{21}	237		215 (w)	δ(Mo-O_{2c2}-Mo)
a_1	ν_7	232		246 (s)[a]	ν_s(Mo-O_{4c}), δ(Mo-O_{2c2}-Mo),
t_2	ν_{59}	200 (4)		203 (w)	δ(Mo-O_{2c2}-Mo)
t_2	ν_{60}	189 (4)		169 (w)	δ(O_{2c1}-Mo-O_t)
t_2	ν_{61}	150 (0)		154 (w)	δ(Mo-O-Mo), δ(O-Mo-O)
a_1	ν_8	108		109 (s)	δ(O_{2c1}-Mo-O_t)
t_2	ν_{63}	79 (2)		84	δ(Mo-O-Mo), δ (O-Mo-O)

[a] Reported as polarized in DMF solution.

Although there is a significant improvement in the agreement between the calculated and observed vibrational frequencies, the assignments of the key vibrational bands described in my previous work[18] and the approximate description of the vibrations is unchanged. Hence, only a brief description of the pertinent features will be discussed here. Lyhamn and co-workers[27] in their normal coordinate analyses of the Keggin anions considered the internal motions of the $[M_3O_{13}]$ units as ligands around the central XO_4 tetrahedron linked together by the bridging O_{2c2} groups. In this approach, the vibrations of the $[M_3O_{13}]$ give rise to "ligand vibrations" and the linking with the bridging groups to "interligand vibrations". With a properly defined force-field, this method, of course, yields the same results as a complete molecule approach. The approach was reported to be a useful method of analyzing the atomic motions and for comparing the spectroscopic features of the α- and β-isomers. An essentially equivalent approach was used to explain the similarities in the vibrational spectra of the α- and β-isomers at a qualitative level by Rocchiccioli-Deltcheff et al.[9]

As in my previous analysis,[18] the highest frequency IR band, observed at 1063 cm^{-1}, corresponds to asymmetric stretching of the P–O and Mo–O_t bonds. The observed and calculated intensity of this band is quite low and this is initially surprising given the assignment. The motions of the P–O and Mo–O_t bonds are themselves coupled asymmetrically such that the dipole moment produced, and hence the intensity of the band, is quite low despite the large polarity associated with the individual bonds. In contrast, the symmetric coupling of these motions leads to the intense band (ν_{45}) at about 972 cm^{-1} assigned to the very strong band observed at 955 cm^{-1}. The weak feature at around 1100 cm^{-1} in the experimental IR spectrum, and which also appears in that of the β-isomer, appears to be due to an impurity as no calculated peak is present in this region.

The IR band at 998 cm^{-1}, observed as an intense shoulder on the band at 955 cm^{-1}, is assigned as the ν_{as} (Mo–O_t) (ν_{44}) motion. The strong IR band at about 880 cm^{-1} is assigned to an asymmetric stretch of the Mo-O_{2c2}-Mo bonds (ν_{46}), calculated to lie at 904 cm^{-1}, involving the movement of the $[Mo_3O_{13}]$ units with almost no internal motion of these groups and so can be classified as an "interligand vibration" as described by Lyhamn and co-workers[27] and Thouvenot et al.[10] The very strong band at about 805 cm^{-1} is similarly

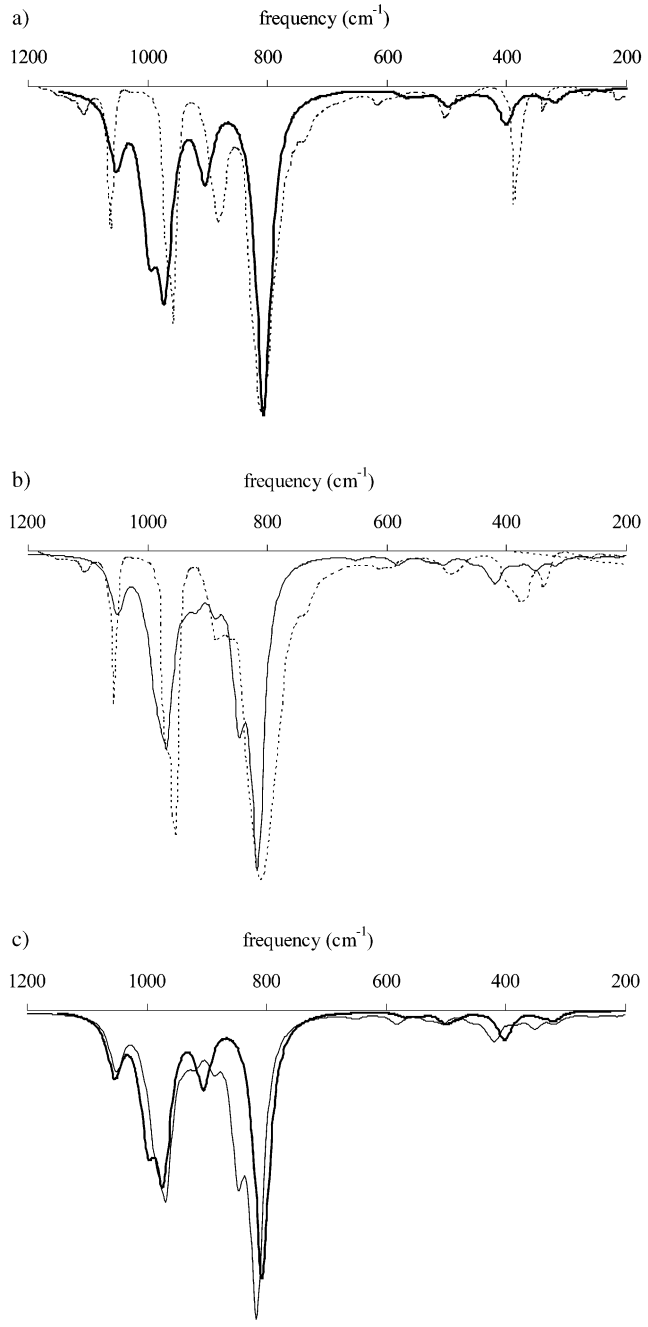

Figure 3. Comparison of the IR spectra for the α- and β-isomers of $[PMo_{12}O_{40}]^{3-}$: a) calculated (——) and observed (-----) spectral traces for α-$[PMo_{12}O_{40}]^{3-}$, b) calculated (——) and observed (-----) spectral traces for β-$[PMo_{12}O_{40}]^{3-}$, and c) calculated spectral traces for α- (——) and β-$[PMo_{12}O_{40}]^{3-}$ (-----). The observed traces have been constructed from those of Thouvenot et al.[10] by converting transmittance to relative absorbance, assuming 5% transmittance for the strongest band.

assigned to the calculated intense peak at 806 cm^{-1} (ν_{47}) corresponding to the internal "ligand" asymmetric stretch of the Mo-O_{2c1}-Mo bonds within the $[Mo_3O_{13}]$ units with very little "interligand" character.

The highest frequency, polarized Raman band lies at about 986 cm^{-1} can readily be assigned to the symmetric stretch of the Mo–O_t bonds (ν_1), calculated to lie at 1016 cm^{-1}. The ν_s (P–O) mode (ν_2) is predicted to occur at 948 cm^{-1} and the absence of a polarized band in the Raman spectrum in this region appears to be due to a small element of ν_s (Mo-O_t) in this motion, coupled asymmetrically to the P–O stretching motion. The Raman bands at about 971 and 964 cm^{-1} are assigned to asymmetric Mo–O_t stretching motion (ν_{14} and ν_{44} respectively). The Raman band at 894 cm^{-1} is assigned as an asymmetric stretch of the Mo-O_{2c2}-Mo bonds (ν_{46}), calculated to lie at 904 cm^{-1}, which as noted above can be classified as an "interligand vibration". The polarized Raman band at about 603 cm^{-1} is assigned as a combined stretching and bending motion of the Mo-O_{2c1}-Mo bonds of the $[Mo_3O_{13}]$ groups (ν_3). In the present work, the frequency of this band is calculated to be 631 cm^{-1}—a considerable improvement from the value of 532 cm^{-1} calculated in my previous study.[18] The polarized Raman band at about 246 cm^{-1} is assigned to a motion involving symmetric stretching of the Mo–O_{4c} bonds and bending of the "intraligand" Mo-O_{2c2}-Mo bonds (ν_7).

Table 3 lists the calculated and experimental frequencies and assignments for the assigned bands of β-$[PMo_{12}O_{40}]^{3-}$, together with calculated intensities. A full list of calculated frequencies and a description of the character of the vibrations is available in the Supporting Information. Figure 3b shows a graphical comparison between the calculated IR spectrum and that observed experimentally.[10] Figure 3c shows a comparison between the calculated IR traces for the α- and β-isomers. The calculated bands for the β-isomer appear to be shifted further from those of the α-isomer than is observed experimentally. The origin of this is unclear but may be related to the neglect of the solvent in these calculations which is liable to have a greater effect on the β-isomer due to its dipole moment.

As discussed above, the lower symmetry of the β-isomer leads to a large increase in the number of IR-active bands due both to the relaxation of the selection rules and to the splitting of the t_2 and t_1 bands. However, it is clear from the calculated and experimental results that the expected increase in complexity is not realized. The splitting of the ν_{as} (P–O) mode, calculated to lie at 1053 cm^{-1} in the α-isomer, is predicted to be only 6 cm^{-1} with no appreciable shift in the band position, suggesting that the local T_d electronic environment of the $[PO_4]$ unit is conserved in the β-isomer. An unresolved splitting is also predicted for the strong IR band at ca. 955 cm^{-1} due to ν_{as} (Mo–O_t). The intense and polarized Raman band at 986 cm^{-1} in the α-isomer, assigned to a symmetric stretch (a_1 ν_1) is predicted to be shifted by only about 4 cm^{-1} in β-isomer. The high frequency region, dominated by Mo–O_t and P–O stretching modes, is thus very similar for the two isomers, consistent with the small changes predicted in the length of these bonds. As suggested above, the weak feature at around 1100 cm^{-1} in the experimental IR spectrum appears to be due to an impurity.

Larger differences are predicted for the strongest IR band found at 805 cm^{-1} in the α-isomer and assigned as an asymmetric stretch (ν_{47}) of the Mo–O_{2c1} bonds with an asymmetric stretch (ν_{46}) of the Mo–O_{2c2} bonds assigned as a shoulder on the high frequency side. For the β-isomer, the former is predicted to split by about 32 cm^{-1} into a_1 (ν_7) and e (ν_{60}) modes, consistent with the appearance of a shoulder on the

Table 3. Calculated and experimental vibrational frequencies (in cm^{-1}) and approximate descriptions for the assigned bands of β-$[PMo_{12}O_{40}]^{3-}$. The calculated IR intensities ($km\,mol^{-1}$) and an indication (vs = very strong, s = strong, m = medium, w = weak, vw = very weak, sh = shoulder) of the relative intensity in the experimental IR and Raman spectra is also given.

Mode		Calcd	Observed[9,10]		Assignment
			IR	Raman	
a_1	ν_1	1055 (170)	}1056 (s)		ν_{as}(P–O′, P–O), ν_{as}(Mo′–O_t′)
e	ν_{52}	1049 (280)			ν_{as}(P–O), ν_{as}(Mo–O_t)
a_1	ν_2	1012 (10)		988 (vs)[a]	ν_s(Mo–O_t, Mo′–O_t′)
e	ν_{53}	1002 (90)			ν_{as}(Mo–O_t, Mo′–O_t′)
e	ν_{54}	986 (380)	}987 (sh)		ν_{as}(Mo′–O_t′, Mo′–O_t′)
a_1	ν_3	983 (420)			ν_{as}(Mo–O_t, Mo′–O_t′)
e	ν_{55}	978 (50)	965 (sh)	968 (m)	ν_{as} (Mo–O_t, Mo′–O_t′)
a_1	ν_4	967 (590)	}953 (s)		ν_{as}(P–O, P–O′), ν_{as}(Mo–O_t, Mo′–O_t′)
e	ν_{56}	966 (706)		950 (sh)	ν_{as}(P–O, P–O′), ν_{as}(Mo–O_t)
a_1	ν_6	887 (430)	882 (m)	885 (w)	ν_{as}(Mo-O_{2c2}-Mo, Mo′-O_{2c2}′-Mo′)
a_1	ν_7	847 (1800)	863 (m)		ν_{as}(Mo-O_{2c1}-Mo, Mo′-O_{2c1}′-Mo′), ν_{as}(Mo-O_{2c2}-Mo, Mo′-O_{2c2}′-Mo′)
e	ν_{60}	815 (1980)	804 (vs)		ν_{as}(Mo-O_{2c1}-Mo), ν_{as}(Mo′-O_{2c2}′-Mo′)
a_1	ν_8	581 (130)	595 (w)	605 (m)[a]	ν_s(Mo-O_{2c1}-Mo, Mo′-O_{2c1}′-Mo′)
e	ν_{69}	504 (50)	488 (w)		δ(Mo-O_{2c1}-Mo, Mo′-O_{2c1}′-Mo′)
a_1	ν_{14}	425 (60)	401 (w)		δ(Mo-O_{2c1}-Mo, Mo′-O_{2c1}′-Mo′)
e	ν_{74}	382 (45)	378 (m)	363 (vw)	δ(Mo-O_{2c1}-Mo, Mo′-O_{2c1}′-Mo′), δ(Mo-O_{2c2}-Mo, Mo-O_{2c2}′-Mo′)
a_1	ν_{18}	350 (130)	339 (m)		δ(Mo-O_{2c1}-Mo, Mo′-O_{2c1}′-Mo′), δ (Mo-O_{2c2}-Mo, Mo-O_{2c2}′-Mo′)
a_1	ν_{19}	311 (20)		300 (vw)	δ(Mo-O_{2c1}-Mo, Mo′-O_{2c1}′-Mo′), δ(O_{2c1}-Mo-O_t, O_{2c1}′-Mo′-O_t′)
a_1	ν_{21}	249 (20)		244 (s)[a]	ν_s(Mo-O_{4c}, Mo′-O_{4c}′), δ(O-Mo-O, O′-Mo′-O′, O-Mo′-O′)

[a] Reported as polarized in DMF solution.

band experimentally. As noted above, the main structural differences between the isomers occur in the different environments of the O_{2c2} atoms. In the α-isomer, the O_{2c2} atoms are all involved in the "2–2" junctions (Figure 1c). In the β-isomer, however, the $O_{2c2'}$ atoms, which connect the rotated $[M_3O_{13}]$ to the rest of the cluster, are involved in the "2–1" junctions (Figure 2c), so that two distinct types of Mo–O_{2c2} bonds are present. The asymmetric stretching mode of the Mo–O_{2c2} bonds (ν_{46} in the α-isomer) is split by about 80 cm^{-1} into a_1 (ν_6) and e (ν_{56}) modes. The Raman band at about 885 cm^{-1} is assigned to the ν_6 mode. The polarized Raman band at about 605 cm^{-1} is assigned as a combined stretching and bending motion of the Mo-O_{2c1}-Mo and Mo-O_{2c1}-Mo bonds (ν_8). The frequency of this band is calculated to be 581 cm^{-1} representing a larger decrease from its value of 631 cm^{-1} for the α-isomer than observed experimentally.

The polarized Raman band at about 244 cm^{-1} is assigned to a motion involving symmetric stretching of the Mo–O_{4c} bonds and bending of the "intraligand" Mo-O_{2c2}-Mo bonds (ν_{21}).

The shift of about 17 cm^{-1} predicted for this mode (ν_7 and ν_{21} for the α- and β-isomers, respectively) is again much larger than that observed experimentally. More significant differences in the vibrational frequencies of the α- and β-isomers are calculated for the low frequency region (> 400 cm^{-1}). This region comprises bending vibrations of the Mo-O-Mo bridging bonds of all types. However, as shown in Figure 3c, the low intensity of most of the bands in this region leads to only small apparent changes in the spectra.

The calculated IR spectral traces (Figure 3c) are very similar suggesting that the vibrational spectra cannot be reliably used to assign the structure of Keggin molybdates. As suggested by the descriptions of the assigned vibrations in Tables 2 and 3, it is not appropriate, for the majority of the vibrations, to label them as involving "ligand" or "interligand" bonds. In the region of the spectrum involving motions of the Mo-O-Mo bridging bonds, the vibrations are intimately mixed so that the overall motion involves the whole cluster. The molybdate cluster is sufficiently flexible that the structural change caused by rotation of one $[M_3O_{13}]$ group is spread over the whole molecule. As outlined above, there are only small differences in the geometries of the $[MO_6]$ and $[PO_4]$ units comprising the polyanion and slight weakening of the bonding of the rotated trimetallic unit to the rest of the cluster is compensated by contraction of the bonds within the unit. The "reduced rigidity" of the molybdates framework compared to that in tungstates has been pointed out by Thouvenot et al.[10] who also suggested that, as a result, the tungsten analogues display larger differences in the vibrational characteristics of the α- and β-isomers.

Conclusion

High-level density functional methods have been used to calculate the structure and vibrational frequencies of the α- and β-isomers of $[PMo_{12}O_{40}]^{3-}$. In general, the agreement between the calculated unscaled vibrational frequencies and those determined experimentally is very good, allowing the IR and Raman spectra to be assigned. For the α-isomer, the agreement with experiment using the current level of theory is superior to that obtained previously. For the β-isomer, the agreement with experiment is slightly poorer but still allows the spectrum to be assigned. To calculate the structure and vibrational spectra of these large molydate cluster ions requires large basis sets and a good treatment of electron correlation and relativistic effects. For the 53-atom $[PMo_{12}O_{40}]^{3-}$ ions, the computational demands are very high requiring several months computational time. Such analyses cannot yet be considered a standard task. Reassuringly, the vibrational analyses confirm the high symmetry, T_d and C_{3v} for the α- and β-isomers, respectively, assumed by previous workers in this field.

The calculated IR spectral traces for the two isomers are quite similar so that vibrational spectroscopy is probably not a reliable technique for identifying the isomeric form of molybdates. The similarity of the vibrational characteristics appears to be due to the relative flexibility of the molybdates where the slight weakening of the bonding of the rotated trimetallic unit to the rest of the cluster in the β-isomer is

Table 4. Characteristic group frequencies for type I polyoxometalates.[a] Except where indicated, the frequencies are based on both calculated and observed spectra.

		$[XMo_{12}O_{40}]^{z-}$			$[Mo_6O_{19}]^{2-}$[19]		
		assignment		frequency [cm^{-1}]	assignment	frequency [cm^{-1}]	
		α	β				
ν_{as}(X−O)	IR	ν_{43}	ν_1 and ν_{52}	940–1060			
	IR	ν_{45}	ν_4 and ν_{56}	800–960			
ν_s(Mo−O_t)	R	ν_1	ν_2	960–999	R	ν_1	980–999
ν_{as}(Mo−O_t)	IR	ν_{44}	ν_3 and ν_{53}	920–980	IR	ν_{14}	957–970
ν_{as}(Mo−O_t)	R	ν_{14} and ν_{44}	ν_3, ν_{53} and ν_{54}	920–980	R	ν_6	951–968
ν_s(Mo-O_{2c1}-Mo)	R	ν_3	ν_8	600–630			
ν_{as}(Mo-O_{2c1}-Mo)	IR	ν_{47}	ν_{60}	700–810	IR	ν_{15}	796–810
ν_{as}(Mo-O_{2c2}-Mo)	IR	ν_{46}	ν_6 and ν_7	770–900			
ν_s(Mo−O_a)	R	ν_7	ν_{21}	245–247	R	ν_3	278–290

[a] The atom numbering is defined in Figure 1a and 2a for α- and β-$[XMo_{12}O_{40}]^{z-}$, respectively. For $[Mo_6O_{19}]^{2-}$, the label O_b was used to denote the doubly bridging oxygens equivalent to O_{2c} in reference [19] The label O_a refers to the four coordinate oxygen (O_{4c}) for the Keggin structure and the six-coordinate, central oxygen, labeled O_c in for $[Mo_6O_{19}]^{2-}$.

compensated by contraction of the bonds within the unit and the structure of the $[MO_6]$ and $[PO_4]$ units in the two isomers is nearly identical. The vibrations characteristic of the bridging Mo-O-Mo bonds involve both the "2–2" junctions between rotated $[M_3O_{13}]$ units and the "1–2" junctions between rotated and unrotated units. The separation of "ligand" and "interligand" vibrations is not clear.

Table 4 lists characteristic group frequencies for the Lindqvist and Keggin molybdates. Both of these ions are Type I polyoxometalates in Pope's classification[1] as they contain only a single terminal M−O group on each metal center. As discussed above, Keggin anions contain both edge- and corner-sharing type I octahedra, whilst Lindqvist anions contain only edge-sharing groups.

Acknowledgement

The author would like to the University of Hull for financial support and the UK Computational Chemistry Working Party for access to computational facilities in the Rutherford Appleton Laboratory.

[1] M. T. Pope, *Heteropoly and Isopoly Oxometalates*, Springer, Heidelberg, **1983**.
[2] M. T. Pope, A. Müller, *Angew. Chem.* **1991**, *103*, 56; *Angew. Chem. Int. Ed. Engl.* **1991**, *30*, 34.
[3] L. C. W. Baker, D. C. Glick, *Chem. Rev.* **1998**, *98*, 3.
[4] M. T. Pope, A. Müller, *Polyoxometalates: from Platonic Solids to Anti-Retroviral Activity*, Kluwer, Dordrecht, **1994**.
[5] J. J. Berzelius, *Poggendorfs Ann. Phys. Chem.* **1826**, *6*, 369.
[6] C. Marginac, *Ann. Chim. Phys.* **1864**, *3*, 1.
[7] J. Keggin, *Nature* **1933**, *131*, 908.
[8] K. Yamamura, Y. Sasaki, *J. Chem. Soc. Chem. Commun.* **1973**, 648.
[9] C. Rocchiccioli-Deltcheff, M. Fournier, R. Franck, R. Thouvent, *Inorg. Chem.* **1983**, *22*, 207.
[10] R. Thouvenot, M. Fournier, R. Franck, C. Rocchiccioli-Deltcheff, *Inorg. Chem.* **1984**, *23*, 598.
[11] R. I. Buckley, R. J. H. Clark, *Coord. Chem. Rev.* **1985**, *65*, 167.
[12] M.-M. Rohmer, M. Bénard, J.-P. Blaudeau, J. M. Maestre, J. M. Poblet, *Coord. Chem. Rev.* **1998**, *178–180*, 1019.
[13] X. López, J. M. Maestre, C. Bo, J. M. Poblet, *J. Am. Chem. Soc.* **2001**, *123*, 9571.
[14] J. M. Maestre, X. López, C. Bo, J. M. Poblet, N. Casañ-Pastor, *J. Am. Chem. Soc.* **2001**, *123*, 3749.
[15] J. M. Maestre, X. López, C. Bo, J. M. Poblet, *Inorg. Chem.* **2002**, *41*, 1883.
[16] X. López, C. Bo, J. M. Poblet, *J. Am. Chem. Soc.* **2002**, *124*, 12574.
[17] A. J. Bridgeman, G. G. Cavigliasso, *J. Phys. Chem. A* **2003**, *107*, 6613.
[18] A. J. Bridgeman, *Chem. Phys.* **2003**, *287*, 55.
[19] A. J. Bridgeman, G. Cavigliasso, *Chem. Phys.* **2002**, *279*, 143.
[20] G. te Velde, F. M. Bickelhaupt, E. J. Baerends E. J. , G. Fonseca Guerra, J. G. Snijders, T. Ziegler, *J. Comput. Chem.* **2001**, *22*, 931; C. Fonseca Guerra, J. G. Snijders, G. te Velde, E. J. Baerends, *Theor. Chem. Acc.* **1998**, *99*, 391.
[21] ADF2002.02, SCM, Theoretical Chemistry, Vrije Universiteit, Amsterdam, The Netherlands, http://www.scm.com
[22] Gaussian 98 (Revision A.7), M. J. Frisch, G. W. Trucks, H. B. Schlegel, G. E. Scuseria, M. A. Robb, J. R. Cheeseman, V. G. Zakrzewski, J. A. Montgomery, R. E. Stratmann, J. C. Burant, S. Dapprich, J. M. Millam, A. D. Daniels, K. N. Kudin, M. C. Strain, O. Farkas, J. Tomasi, V. Barone, M. Cossi, R. Cammi, B. Mennucci, C. Pomelli, C. Adamo, S. Clifford, J. Ochterski, G. A. Petersson, P. Y. Ayala, Q. Cui, K. Morokuma, D. K. Malick, A. D. Rabuck, K. Raghavachari, J. B. Foresman, J. Cioslowski, J. V. Ortiz, B. B. Stefanov, G. Liu, A. Liashenko, P. Piskorz, I. Komaromi, R. Gomperts, R. L. Martin, D. J. Fox, T. Keith, M. A. Al-Laham, C. Y. Peng, A. Nanayakkara, C. Gonzalez, M. Challacombe, P. M. W. Gill, B. G. Johnson, W. Chen, M. W. Wong, J. L. Andres, M. Head-Gordon, E. S. Replogle, J. A. Pople, Gaussian, Inc., Pittsburgh, PA, **1998**.
[23] S. H. Vosko, L. Wilk, M. Nusair, *Can. J. Phys.* **1980**, *58*, 1200.
[24] Spectral Plot. A Java applet to plot spectral traces from the output of the electronic structure packages Gaussian98 and ADF, written by A. J. Bridgeman, University of Hull, 2002, http://www.hull.ac.uk/chemistry/plotSpectralData.php
[25] L. H. Bi, E. B. Wang, L. Xu, R. D. Huang, *Inorg. Chim. Acta* **2000**, *305*, 163.
[26] M. Ugalde, J. M. Gutierrez-Zorrilla, P. Vitoria, A. Luque, A. S. J. Wery, P. Roman, *Chem. Mater.* **1997**, *9*, 2869.
[27] L. Lyhamn, S. J. Cyvin, B. N. Cyvin, J. Brunvoll, *Spectrosc. Lett.* **1976**, *9*, 859; L. Lyhamn, S. J. Cyvin, B. N. Cyvin, J. *Z. Naturforsch. Teil A* **1976**, *31*, 1589; L. Lyhamn, S. J. Cyvin, *Spectrosc. Lett.* 1977, *10*, 907; L. Lyhamn, S. J. Cyvin, B. N. Cyvin, J. Brunvoll, *Spectrosc. Lett.* **1979**, *12*, 101; L. Lyhamn, S. J. Cyvin, *Monatsh. Chem.* **1979**, *110*, 311.

Received: December 8, 2003

Published online: April 26, 2004

